

Supporting information

Dependence of fluorination intercalation for graphene toward high-quality fluorinated graphene formation

Kun Fan,^a Jiemin Fu,^a Xikui Liu,^a Yang Liu,^a Wenchuan Lai,^a Xiangyang Liu,^{a} Xu Wang,^{a*}*

^a College of Polymer Science and Engineering, State Key Laboratory of Polymer Material and Engineering, Sichuan University, Chengdu 610065, People's Republic of China.

*Authors to whom any correspondence should be addressed.

Corresponding author *Tel.:+86 28 85403948. Fax: +86 28 85405138.

E-mail address: lxy6912@sina.com(Xiangyang Liu), wangxu@scu.edu.cn(Xu Wang);

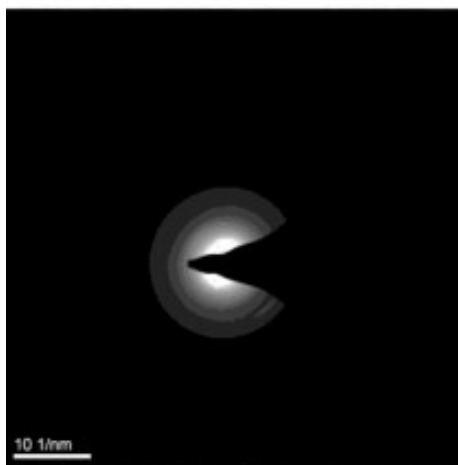


Figure S1. Selected area electron diffraction (SAED) image of OG sample

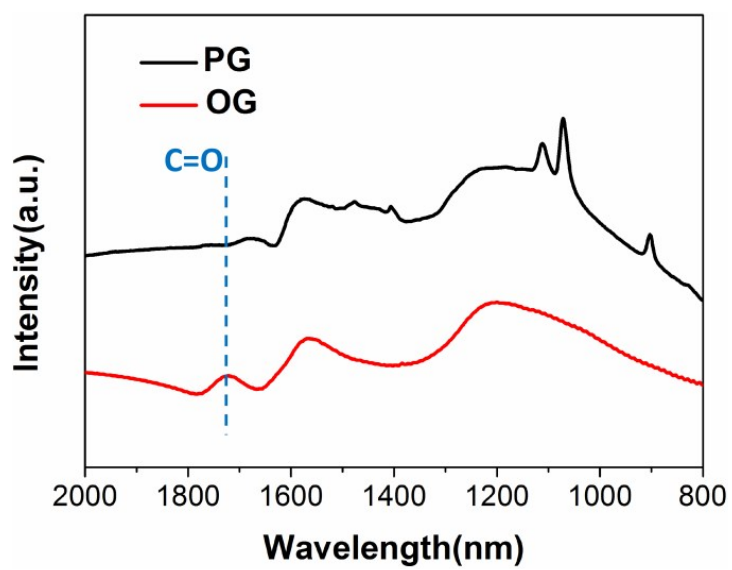


Figure S2. FTIR spectra of PG and OG samples

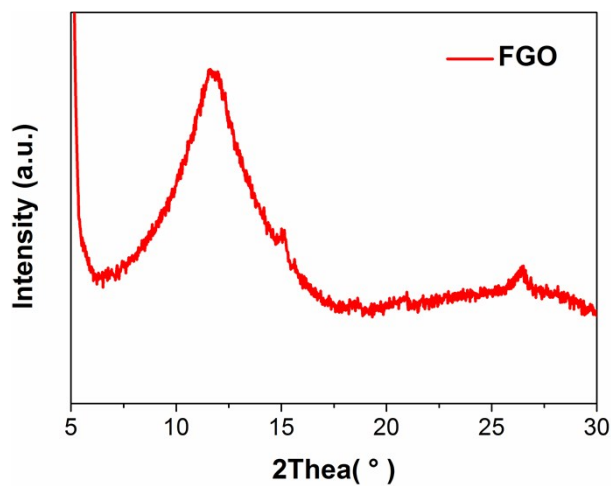


Figure S3. XRD pattern of FGO sample.

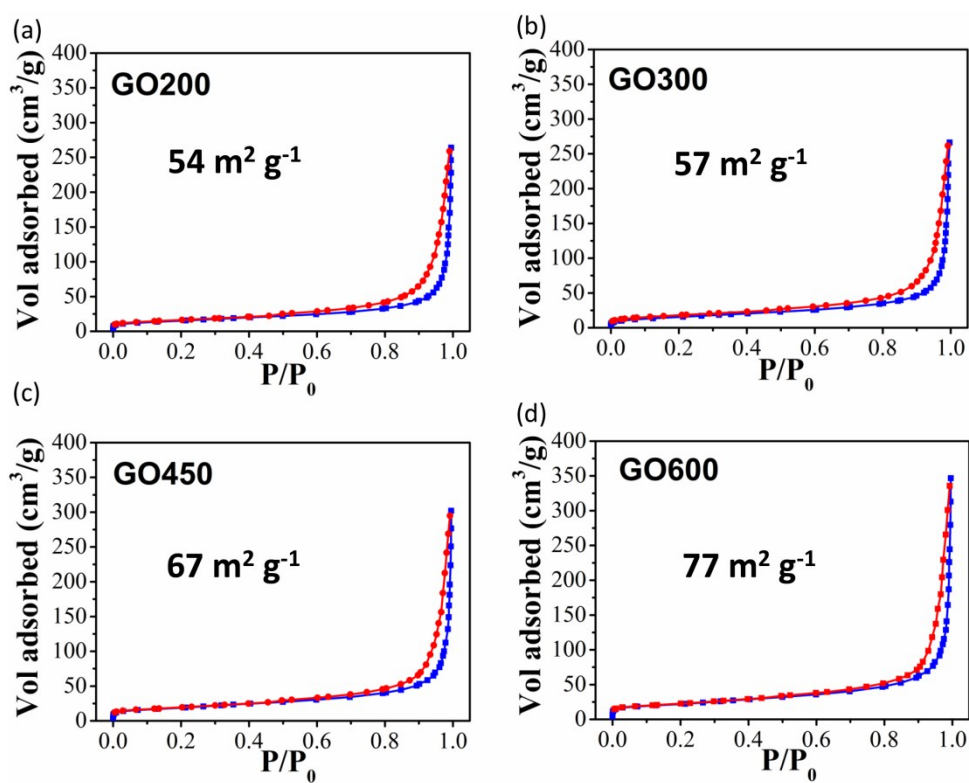


Figure S4. Nitrogen sorption isotherms and the corresponding specific surface areas of different samples (a) GO200 (b) GO300 (c) GO450 (d) GO600

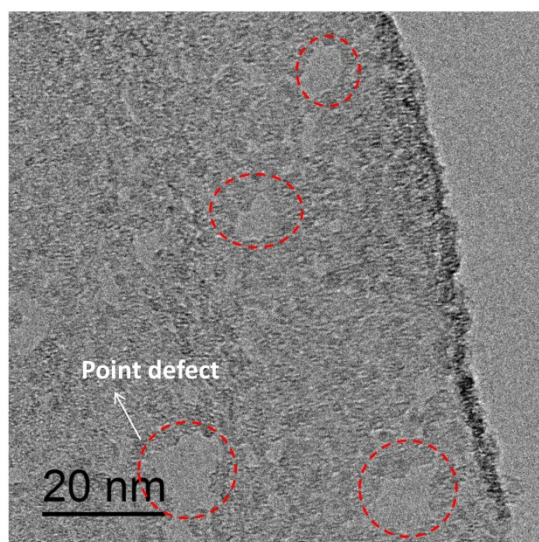


Figure S5. TEM image of GO600 sample

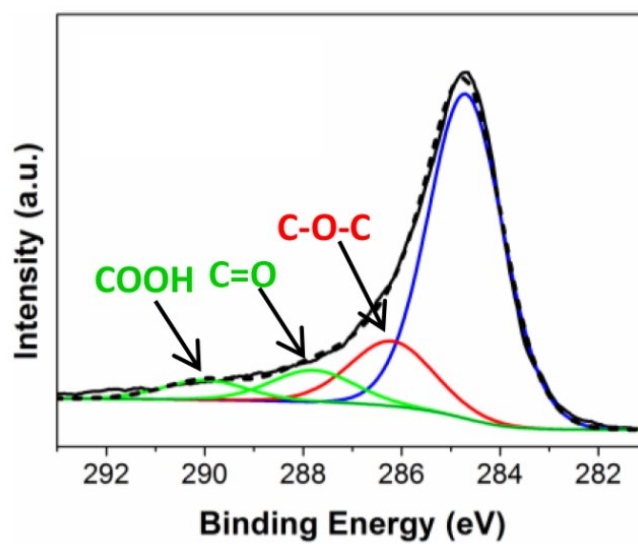


Figure S6. Curve fitted XPS C1s spectrum of OG sample

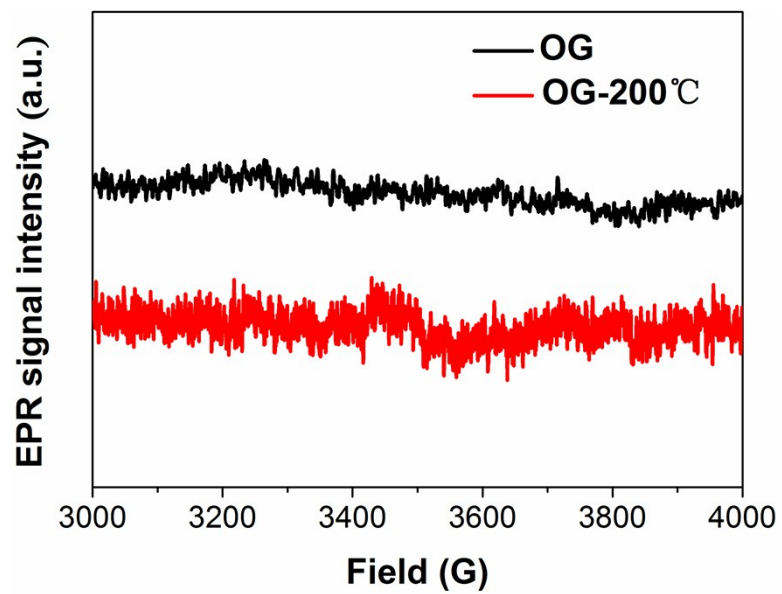


Figure S7. EPR spectra of OG sample and OG sample at 200 °C

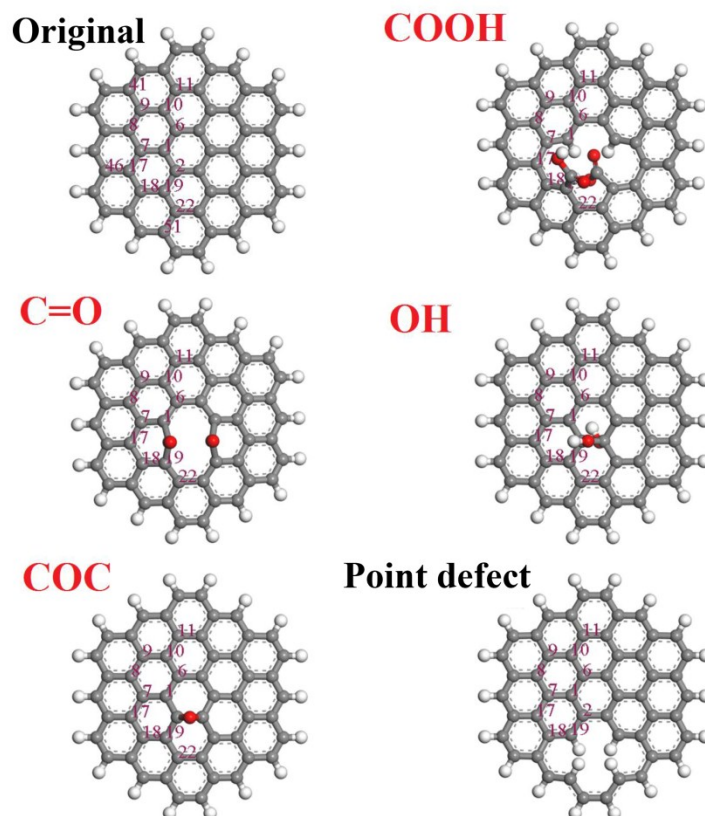


Figure S8. The structures of model molecules with various oxygen groups and point defects

Herein, fluorination reaction between graphene and fluorine gas under high temperature was regarded as radical attack.¹ The CFF indices were compared to estimate the fluorination reactivity for carbons in every group, and the larger value meant greater possibility of suffering radical addition². Considering the complexity of the system, we defined the “average CFF indices” to compare carbons located at aromatic regions and total 12 carbons positions were chose, as shown in Figure S8, which were calculated from all respective CFF indices for a model molecule. Accordingly, the “average CFF indices” of original aromatic regions is 0.00725, and the “average CFF indices” of aromatic regions close to point defects, carbonyl and carboxyl are 0.00669, 0.00797 and 0.00958, respectively.

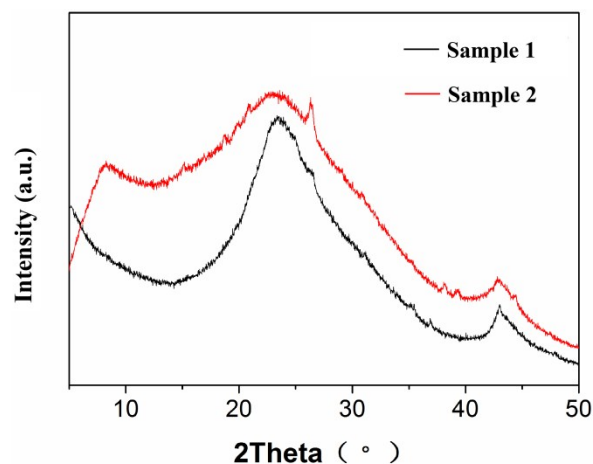
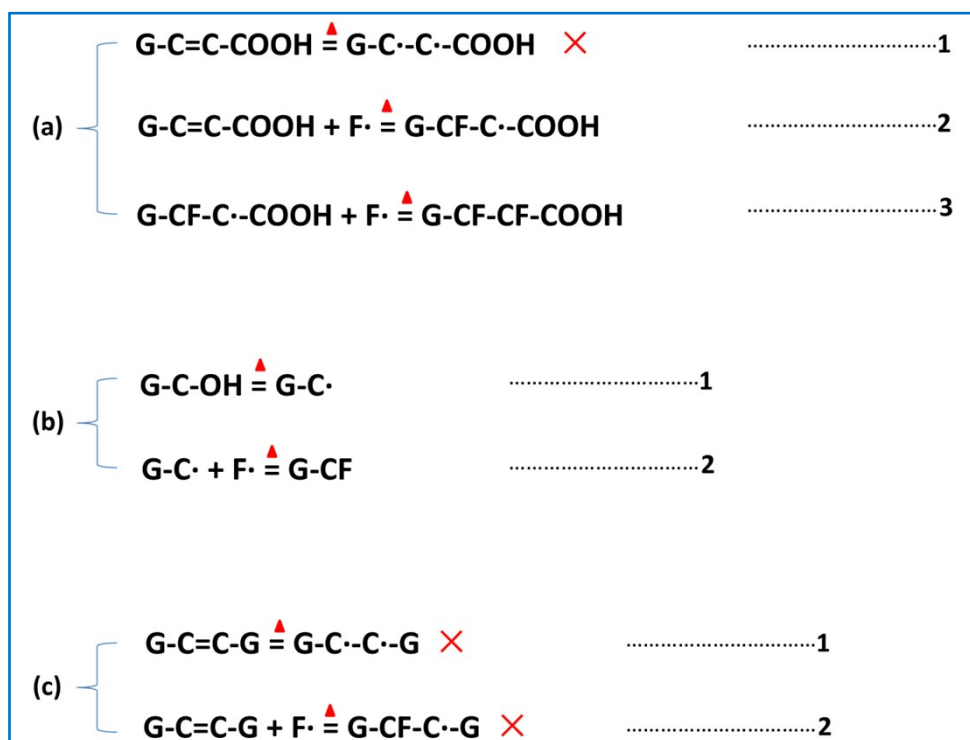


Figure S9. XRD patterns of sample 1 (OG) and sample 2 (fluorination intercalation of OG within 2 min)

As shown in Figure S9, the peak position of sample 2 (fluorination intercalation of OG within 2 min) has little change compared with that of sample 1 (OG), which indicates the interlayer distance of sample 2 has no increase. This result reveals that fluorination intercalation of OG with carbonyl and carboxyl does not occur in a transitory time (within 2 min), so it needs more reaction time compared with that of rapidly produced active radicals from hydroxyl and epoxy groups.



Schematic S1. Fluorination intercalation mechanisms for graphene with (a) –COOH (or C=O) (b) –OH (or epoxy groups) (c) point defects

As shown in Schematic S1a, graphene with –COOH (or C=O) would not produce free radicals under high temperature (stage 1). The generation of free radicals needs a process; that is, the F· attacks the activated aromatic regions by –COOH (or C=O), then free radicals produce (stage 2). Afterwards, the F· can attack produced free radicals again for further fluorination intercalation (stage 3). However, the reaction energy barrier exists in the process of generating free radicals. For graphene with –OH (or epoxy groups) (Schematic S1b), the free radicals can directly produce under high temperature (stage 1), then the F· can easily attack (stage 2). Therefore, fluorination intercalation for –OH (or epoxy groups) should possess lower reaction energy barrier compared with that of –COOH (or C=O). For graphene with point defects (Schematic S1c), it would not produce free radicals under both high

temperature and F· attacking (stage 1 and 2), so it is difficult to perform fluorination intercalation.

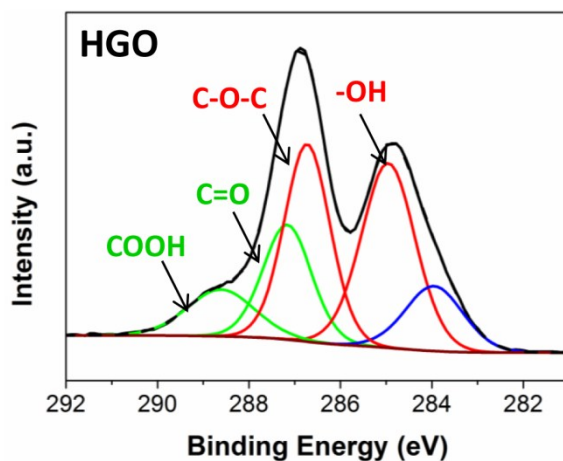


Figure S10. Curve fitted XPS C1s spectra of HGO sample

Table S1. Chemical Compositions of GO and HGO Measured by XPS

Sample	Chemical composition of the samples			
	-OH (content %)	C-O-C (content%)	C=O (content%)	COOH (content%)
GO	16.96	19.80	10.63	3.00
HGO	31.66	28.72	17.69	9.96

Table S2. The chemical composition of FHGO based on XPS calculation

Sample	C content (at%)	O content (at%)	F content (at%)	F/C ratio
FHGO	46.82	8.49	44.69	0.95

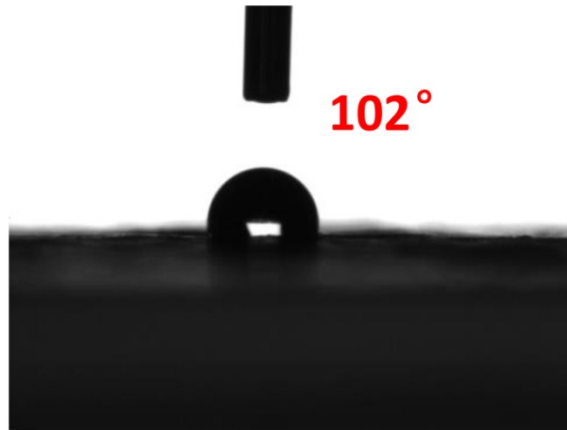


Figure S11. The photograph of water contact angle for OG sample

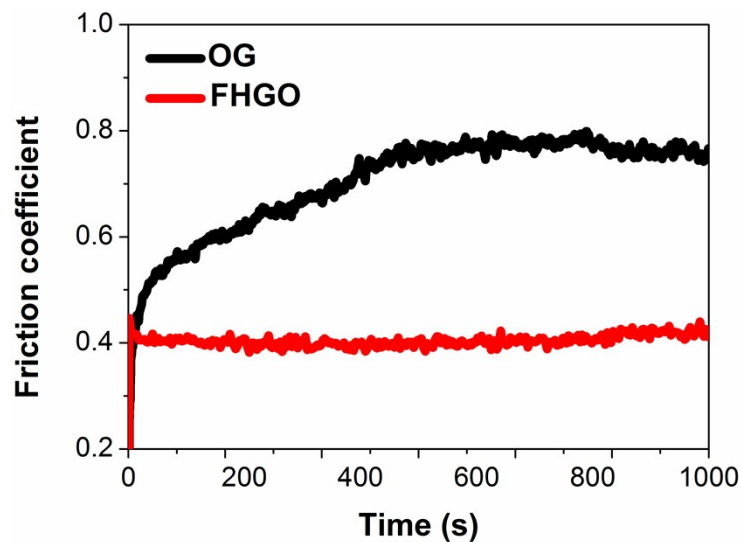


Figure S12. Friction coefficient lines of OG and FHGO solid lubrication films

The preparation of OG and FHGO solid lubrication films refers to LbL self-assembly procedure reported in the literature³. In brief, 0.2 wt% aqueous solution of dopamine firstly treated the substrates (AISI 304, steel) as adhesion layer. Then the substrates were consecutively dipped into a 0.1 mg/ml alcohol solution of OG or FHGO. After drying alcohol, the substrates were again dipped into a 0.1 mg/ml alcohol solution of OG or FHGO. This process was repeated 15 times. In order to

accurately reflect the tribological characteristics of OG and FHGO films, the smaller load (0.1N) was chosen to avoid destroying OG and FHGO films. Because the top-ball would directly contacts the down-substrate with the damaged OG and FHGO films, which leads to the inveracious response for tribological characteristics of OG and FHGO films.

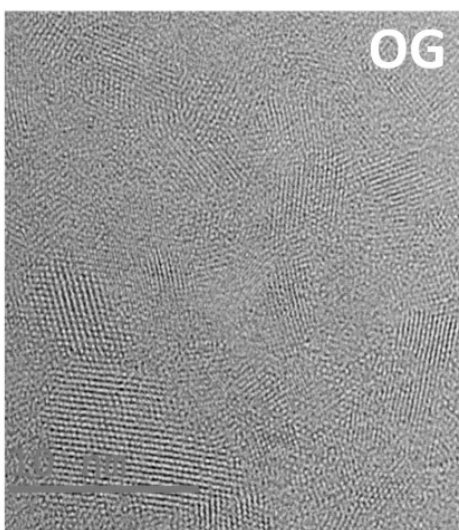


Figure S13. Atomic resolution, AC-TEM image of OG sample

As shown in Figure S13, OG possesses multitudinous and integrated aromatic regions, leading to strong π - π stacking effect, so commensurate stacking between graphene sheets would form. They explained the shearing process with a higher energy cost by DFT calculations. As shown in Figure 6a in the manuscript, in original state (1 position), graphene sheet stacks each other in a commensurate position by interlayer π - π stacking effect, presenting a high stability by this way. In order to change this state, a big enough shear force needs to apply on top-graphene sheet. Then, it begins to move on the surface of down-graphene sheet, thereby coming into an

incommensurate position (2 position). However, transformation from incommensurate to commensurate position on graphene sheet is a superlubric pathway, namely a spontaneous process without any external force. From 2 to 3 position, it is easy for graphene stacking to return to a commensurate position. This process reveals that it is difficult for graphene to exfoliate by shearing process, while the phenomenon would not occur in peeling process. Therefore, the shearing process is disadvantageous to exfoliate graphene.

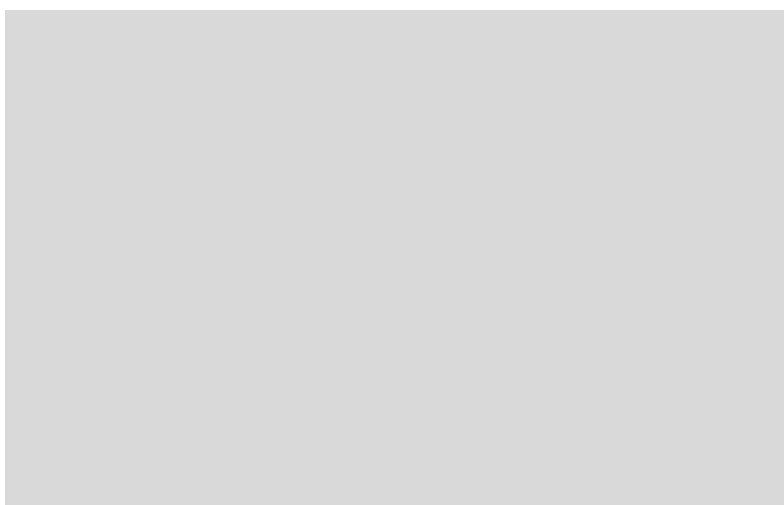


Figure S14. Atomic resolution, AC-TEM images of FHGO sample

For FHGO, the highly effective fluorination intercalation has almost completely destroyed the aromatic regions of graphene, namely from sp^2 carbon skeleton to sp^3 carbon skeleton, and only minimal aromatic regions were reserved, as shown in Figure S14.

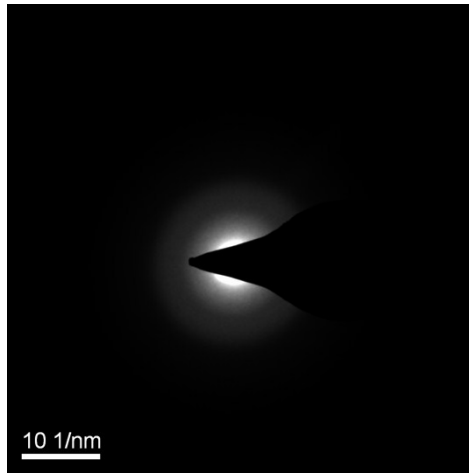


Figure S15. Selected area electron diffraction (SAED) image of FHGO sample

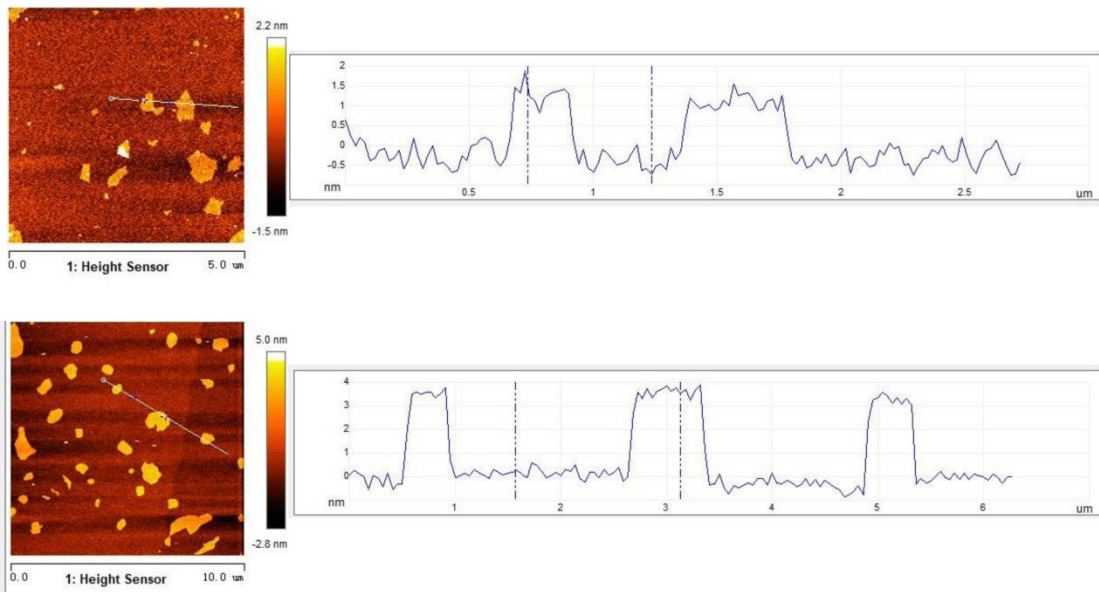


Figure S16. AFM images of exfoliated FHGO sample

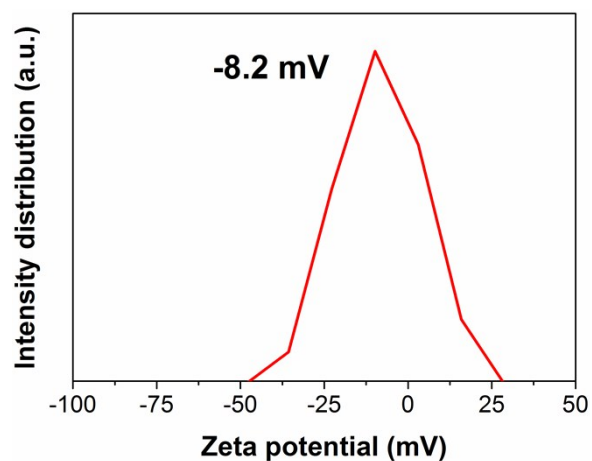


Figure S17. Zeta potential of graphene sheet

References:

- (1) Lai, W, Wang, X, Fu, J, Chen, T, Fan, K, Liu, X, Radical Chain Reaction Mechanism of Graphene Fluorination. *Carbon* **2018**, *137*, 451-457.
- (2) Lai, W, Wang, X, Li, Y, Liu, Y, He, T, Fan, K, Liu, X, The Particular Phase Transformation During Graphene Fluorination Process. *Carbon* **2018**, *132*, 271-279.
- (3) Saravanan, P, Selyanchyn, R, Tanaka, H, Fujikawa, S, Lyth, SM, Sugimura, J, Ultra-Low Friction Between Polymers and Graphene Oxide Multilayers in Nitrogen Atmosphere, Mediated by Stable Transfer Film Formation. *Carbon* **2017**, *122*, 395-403.